

RESEARCH

Open Access



Tobacco and menthol flavored nicotine-free electronic cigarettes induced inflammation and dysregulated repair in lung fibroblast and epithelium

Qixin Wang¹, Joseph H Lucas¹, Cortney Pang¹, Ruogang Zhao² and Irfan Rahman^{1*}

Abstract

Background Electronic cigarette (e-cig) vaping has increased in the past decade in the US, and e-cig use is misleadingly marketed as a safe cessation for quitting smoking. The main constituents in e-liquid are humectants, such as propylene glycol (PG) and vegetable glycerine (VG), but different flavoring chemicals are also used. However, the toxicology profile of flavored e-cigs in the pulmonary tract is lacking. We hypothesized that menthol and tobacco-flavored e-cig (nicotine-free) exposure results in inflammatory responses and dysregulated repair in lung fibroblast and epithelium.

Method We exposed lung fibroblast (HFL-1) and epithelium (BEAS-2B) to Air, PG/VG, menthol flavored, or tobacco-flavored e-cig, and determined the cytotoxicity, inflammation, and wound healing ability in 2D cells and 3D microtissue chip models.

Results After exposure, HFL-1 showed decreased cell number with increased IL-8 levels in the tobacco flavor group compared to air. BEAS-2B also showed increased IL-8 secretion after PG/VG and tobacco flavor exposure, while menthol flavor exposure showed no change. Both menthol and tobacco-flavored e-cig exposure showed decreased protein abundance of type 1 collagen α 1 (COL1A1), α -smooth-muscle actin (α SMA), and fibronectin as well as decreased gene expression level of α SMA (*Acta2*) in HFL-1. After tobacco flavor e-cig exposure, HFL-1 mediated wound healing and tissue contractility were inhibited. Furthermore, BEAS-2B exposed to menthol flavor showed significantly decreased tight junction gene expressions, such as *CDH1*, *OCLN*, and *TJP1*.

Conclusion Overall, tobacco-flavored e-cig exposure induces inflammation in both epithelium and fibroblasts, and tobacco-flavored e-cig inhibits wound healing ability in fibroblasts.

Keywords Menthol, Nicotine-free, Tobacco, Repair, Injury, Inflammation, ENDS

*Correspondence:

Irfan Rahman

irfan_rahman@urmc.rochester.edu

¹Department of Environmental Medicine, University of Rochester Medical Center, 601 Elmwood Avenue, Box 850, Rochester, NY 14642, USA

²Department of Biomedical Engineering, University at Buffalo, Buffalo, NY 14260, USA



© The Author(s) 2023. **Open Access** This article is licensed under a Creative Commons Attribution 4.0 International License, which permits use, sharing, adaptation, distribution and reproduction in any medium or format, as long as you give appropriate credit to the original author(s) and the source, provide a link to the Creative Commons licence, and indicate if changes were made. The images or other third party material in this article are included in the article's Creative Commons licence, unless indicated otherwise in a credit line to the material. If material is not included in the article's Creative Commons licence and your intended use is not permitted by statutory regulation or exceeds the permitted use, you will need to obtain permission directly from the copyright holder. To view a copy of this licence, visit <http://creativecommons.org/licenses/by/4.0/>. The Creative Commons Public Domain Dedication waiver (<http://creativecommons.org/publicdomain/zero/1.0/>) applies to the data made available in this article, unless otherwise stated in a credit line to the data.

Background

Electronic nicotine delivery systems (ENDS), also known as electronic cigarettes (e-cigs) are devices that generate aerosols to mimic cigarette smoking, and e-cigs are marketed broadly as a smoking cessation tool [1–4]. The e-liquid mixture usually contains humectants, nicotine, and other additives. The humectant used in e-liquid is a mixture of propylene glycol (PG) and/or vegetable glycerin (VG), which are substances generally recognized as safe (GRAS). Other additives added to e-liquids include different flavoring chemicals, initially added to improve the taste and ease the throat hit, but unexpectedly attracted younger generations [5]. In 2022, around 2.5 million high-school and middle-school students were active e-cig users, and 85% of products were flavored e-cigs [6]. Although the FDA issued series of policies to regulate different flavored e-cigs in 2020, tobacco and menthol-flavored e-cigs are still available on the market in some States, which showed an unexpected increase in consumption after the flavor ban [7]. Since nicotine is an addictive substance in e-liquid, various vendors have provided nicotine-free e-cigs with fruit, menthol and tobacco-flavored e-cigs and advertised them as non-addictive products for smoking cessation. There are studies reported that hazardous chemical emissions from e-cig aerosol, such as formaldehyde and acetals, released from atomized PG/VG [8, 9], and diacetyl, acetoin, maltol, or eugenol are associated with tobacco flavorants [10–12]. Harmful chemicals are released without the presence of nicotine in e-cig, and previous reports have shown that e-cig aerosol without nicotine produced lung inflammatory responses, impaired lung functions, and dysregulated tissue repair [13–16]. We also found that 1-month e-cig exposure showed dysregulated expressions of matrix metalloproteinases (MMPs), A disintegrin and metalloprotease (ADAMs), and collagens which are responsible for extracellular matrix (ECM) remodeling, wound healing, and repair [13, 14, 16]. Although studies showed that e-cig exposure induced inflammatory responses and potential dysregulated repair, no study currently focuses on how menthol and tobacco-flavored e-cigs cause dysregulated wound healing.

Wound healing in the lung is usually initiated after injury on the lung epithelium, and lung fibroblasts migrate to the injury site and accelerate epithelial repair [17]. Considering e-cig vaping is a constant habit, other environmental hazards, such as viral infection, might occur during e-cig vaping. Dysregulated wound healing due to e-cig exposure could be one of the reasons for lung injury exacerbation, as our prior report shows that e-cig vaping augments IAV infection-induced lung injury [18–20]. Lung fibroblasts play a critical role in tissue wound healing and repair, differentiating from fibroblast to myofibroblast during the repair process, which will be

accompanied by overexpression of ECM components, such as collagen, fibronectin and α -smooth muscle actin (α SMA). The overexpressed ECM components increase tissue contractility and generate new ECM that could support the epithelium and accelerate the epithelium repair [17, 21]. Our previous studies showed that flavored e-cig exposure or nicotine treatment inhibited TGF- β induced fibroblast differentiation and induced premature senescence and inflammatory response in a dose-dependent manner [22, 23]. No study focused on how menthol and tobacco-flavored e-cigs (nicotine free) affect the wound healing process mediated by lung fibroblast, which is especially important since menthol and tobacco-flavored e-cig are currently the only legally allowed e-cigs on the market.

We hypothesized that menthol and tobacco-flavored e-cig (nicotine-free) exposure induces inflammatory responses and inhibits wound healing. We exposed human lung fibroblast (HFL-1) and human bronchial epithelial cell (BEAS-2B) to PG/VG, PG/VG+Menthol, and PG/VG+Tobacco flavor to determine the impact of how flavored e-cig, nicotine excluded, exposure disrupts wound healing mediated by lung fibroblast and the inflammatory response from both lung fibroblast and epithelium. We also applied a microtissue chip that can reflect the altered contractility of fibroblast during wound healing response following e-cig exposure.

Methods

Cell culture

Human fetal lung fibroblast (HFL-1, Cat#: CCL-153) and human bronchial epithelial cell (BEAS-2B, Cat#: CRL-9609) were purchased from the American Type Culture Collection (ATCC) and maintained in DMEM/F12K medium with 10% FBS (Cat#: 10,082,147; Thermo Fisher Scientific) for HFL-1, and 5% FBS for BEAS-2B, and total 1% Penicillin-Streptomycin-Glutamine (Cat#: 103-78016; Thermo Fisher Scientific) with 5% CO₂ and 95% humidity. HFL-1 and BEAS-2B were seeded at 30,000 cells/cm² in 6 well plates for 1 day, and HFL-1 were starved in FBS-free medium while BEAS-2B were in 1% FBS medium overnight. Then, the cells were exposed to air, PG/VG (50:50), PG/VG+menthol flavor (nicotine free), and PG/VG+tobacco flavor (nicotine free) the next day. After exposure, cells were either lysed for protein and RNA isolation or fixed with ice-cold methanol for immunofluorescence staining.

E-cig device, e-liquids, and e-cig exposure

The e-cig device used is the Joytech eVIC VTCmini with a 0.15 Ω atomizer/coil (Kanger Tech). The e-liquids containing PG/VG (50:50), PG/VG+menthol flavor (nicotine free), and PG/VG+tobacco flavor (nicotine free) were procured from a local vendor. The air pump, connecting

tubing, and atomizers were changed in between groups. E-cig aerosol was generated and pumped into an EnzyScreen chamber at a rate of 2 puffs per minute for 2 min, and another 8 min were allowed for the e-cig aerosol to deposit. The puffing profile was based on the realistic topography with 3.3s/puff, 26.7s interval, and 70mL puff volume based on the clinical puffing profile [24]. A total of 4 puffs of e-cig aerosol will be exposed to cells, and then cells will be cultured for 2 or 3 days without e-cig aerosols existence. This in vitro exposure model aims to understand that one-time acute aerosol exposure mediated cellular toxicity and wound healing dysregulation.

ELISA

After 2 days of exposure, the conditioned medium was collected and stored at -80 °C. The levels of IL-6 (Catalog# CHC1263, Thermo Fisher Scientific) and IL-8 (Catalog# CHC1303, Thermo Fisher Scientific) were detected in the conditioned medium from both HFL-1 and BEAS-2B, while TGF- β (Catalog# DY240, R&D System) was detected only in HFL-1, according to the manufacturer's protocols.

RNA isolation and qRT-PCR

After 2 days of exposure, cells were washed with PBS twice, and lysed in 700 μ L QIAzol reagent (Cat#:79,306, Qiagen) for 15 min at room temperature, then collected into a 1.7mL tube. Then, 150 μ L chloroform was added to the sample, and vortexed for 10s. The mixtures were centrifuged at 20,000 g for 15 min at 4 °C. The aqueous phase was transferred to a new tube, and 200 μ L of isopropanol was added to the samples and mixed gently. The mixtures were incubated at -20 °C for 3 h, and then spun down at 20,000 g for 15 min at 4 °C. After removing the isopropanol, the RNA pellets were washed with 75% EtOH, and then centrifuged at 20,000 g for 15 min at 4 °C. The EtOH was removed, and the RNA pellet was resuspended with RNase-free water. RNA concentration and quality were checked by Nano-drop spectrophotometer (ND-1000, NanoDrop Technologies). A total of 200 ng of RNA was used for reverse transcription via RT2 First Strand Kit (Cat# 330,401, Qiagen). Synthesized cDNA was diluted 6 times, and used for real-time PCR quantification by using SYBR green expression master-mix (Cat# 330,509, Qiagen) in BioRad CFX96 qPCR machine. All the primers were purchased from BioRad: *COL1A1* (Human, qHsaCEP0050510), *ACTA2* (Human, qHsaCIP0028813), *FNI* (Human, qHsaCEP0050873), *CDH1* (Human, qHsaCID0015365), *CDH2* (Human, qHsaCID0015189), *VIM* (Human, qHsaCED0042034), *TJPI* (Human, qHsaCID0018062), *OCN* (Human, qHsaCED0038290), *SERPINE1* (Human, qHsaCID0006432), and *GAPDH* (Human, qHsaCEP0041396). The thermal cycle for

qRT-PCR was 10 min at 95 °C, then 95 °C, 15 s, and 60 °C, 1 min for 40 cycles, with fluorescence intensity measurement at the end of 1 min incubation at 60 °C. The melting curve was performed when the 40 cycles were finished. The raw Ct value will be used, and the relative change fold will be calculated via $2^{-\Delta\Delta Ct}$ methods with *GAPDH* as the housekeeping gene.

Protein isolation and western blot

Cells were lysed in RIPA buffer and isolated protein was quantified by Pierce BCA Assay Kit (Cat#: 23,227, Thermo Fisher Scientific). Total 20 μ g of protein was loaded in each lane, and run through 10% sodium dodecyl sulfate-polyacrylamide gel electrophoresis (SDS-PAGE). The protein was then transferred onto a nitrocellulose membrane (Cat# 1,620,112, BioRad). The membrane was washed with Tris-buffered saline containing 0.1% Tween 20 (TBS-T) for 10 min, and then blocked with 5% non-fat milk for 1 h at room temperature. Primary antibodies: anti-Fibronectin (1:1000, ab, Abcam), Anti- α -Smooth Muscle Actin (α -SMA) (1:1000, A2547, Sigma), anti-COL1A1 (1:1000, NBP1-30054, Novus Biologicals), anti-vimentin (1:1000, ab92547, Abcam), anti-E-Cadherin (1:1000, 3195, Cell Signaling), anti-N-Cadherin (1:1000, ab76011, Abcam), Anti-Occludin (1:1000, ab216327, Abcam), anti-ZO1 (1:1000, ab221547, abcam), anti-PAI1 (1:1000, ab222754, abcam), and *GAPDH* (1:1000, ab9482, Abcam), were incubated overnight at 4 °C. The following day, the primary antibody was removed, and the membrane was washed 4 times, 15 min each, with TBS-T. Next, the secondary antibody (goat-anti-rabbit, 1:5000, #1,706,515, BioRad; Rabbit Anti-Mouse, 1:5000, ab6728, Abcam) was incubated for 1 h at room temperature. After, the membrane was washed with TBS-T for 4 times, 15 min each, and then detection of the signal with Pierce ECL Western Blotting Substrate (Cat#: 32,106, Thermo Scientific) via Bio-Rad ChemiDoc MP imaging system was done. ImageLab software (BioRad) was used to normalize the densitometry and calculate the change fold based on the air group. *GAPDH* was used as the endogenous control to normalize for sample variation.

Immunofluorescence staining

Cells after e-cig exposure for 2 days were fixed with pre-chilled (-20 °C) methanol for 10 min at 4 °C, and then washed with TBS for 5 min, 3 times. Then, the cells were blocked with 10% normal goat serum for 1 h at room temperature and incubated with anti-COL1A1 (1:100, NBP1-30054, Novus Biologicals) for 16 h at 4 °C. The primary antibody was removed and then washed with TBS for 4 times, 5 min each, and then incubated with goat anti-rabbit IgG (H+L) secondary antibody Alexa Fluor 488 (1:1000, Catalog # A-11,008, ThermoFisher) for 1 h at room temperature. Cells were washed with TBS for 4

times, 5 min each, and then stained with Hoechst 33,342 (Cat# H3570, Thermo Fisher Scientist) for 10 min. Cells were kept in TBS, and stored at 4 °C in the dark to avoid the light under fluorescence imaging. EVOS fluorescence microscopy was used to visualize the nuclear and stained COL1A1. Image J was used to calculate the corrected total cell fluorescence (CTCF) via following equation: integrated Density (IntDen) – (Area of cells * Mean fluorescence of background). The final results are normalized to individual cells as Fluorescence intensity /cell=CTCF/Cell number.

Wound healing assay

Confluent HFL-1 cells were “scratched” by dragging a 200 µl micropipette tip in a single motion across the center of the well. Only the wells, where cells had well-defined edges were included in the study. Immediately following the scratch, images was taken by Cytation 5 system and then exposed to air, PG/VG, menthol or tobacco-flavored e-cigs. The same scratched area was imaged 24, 48, and 72 h post-exposure. Wound or scratch area was calculated in ImageJ.

Microtissue seeding and contraction force measurement

The microtissue device was a polydimethylsiloxane (PDMS) based micropillar arrays in a P35 petridish. The fabrication of microtissue devices and microtissue seeding were described in our previous study [25]. Briefly, the microtissue device was sterilized with 70% EtOH for 15 min, under UV overnight, then treated with Pluronic F-127 (P2443, Sigma) for 10 min to avoid cell adhesion to the PDMS surface. HFL-1 was mixed with 3 mg/mL collagen type-I (rat tail, Corning) and 10% v/v Matrigel (356,231, CORNING), and BEAS-2B were mixed with 2 mg/mL collagen. The mixtures with cells were then centrifuged with the device together at 1200 RPM for 2 min at 4 °C. The excess mixtures were carefully removed and then polymerized at 37 °C. The device was maintained in the respective culture medium in an incubator with 5% CO² and 95% humidity. The microtissue is fully formed in 2 days of culture, and the bottom and top of the micropillar images were taken before the e-cig exposure and for 2 days post-exposure. The contraction force was determined by the deflection position of the micropillar as described. The contraction force $F=k\delta$, where δ is the deflection distance of both pillars: $\delta = (\delta_1 + \delta_2)/2$, and $k=0.9 \mu\text{N}/\mu\text{m}$, which is the spring constant materials. All the pictures of microtissues were taken with an Olympus CKX41 microscope. The deflection distance of pillars were calculated via ImageJ.

Statistical analysis

All the data were visualized through GraphPad Prism software (V.9.0), and significance was calculated via

one-way ANOVA or student's T-test. All the data were presented as mean±SEM, and $p<0.05$ was considered statistically significant.

Results

Tobacco-flavored e-cig exposure induced inflammation in HFL-1

To understand the cytotoxicity of tobacco and menthol-flavored e-cigs, HFL-1 were exposed to PG/VG, menthol-, and tobacco-flavored e-cig for 2 days. A significantly decreased cell number was noticed following tobacco-flavored e-cig exposure compared to air, and there are gaps among cells (Fig. 1A-B). Although there is a decreased trend of cell number after PG/VG and menthol-flavored e-cig exposure, there is no significant difference compared to the air group (Fig. 1B). Among all groups, there is no significant difference in cell viability (Fig. 1B). A significantly increased IL-8 was noticed after tobacco flavor e-cig exposure, while PG/VG and menthol flavor exposure showed no difference compared to air (Fig. 1C), while no significant difference was detected in the level of IL-6 in the conditioned medium among the different groups (Fig. 1C). We also tested the levels of TGF-β released in condition medium among the different groups, no significant difference was found (Fig. 1C).

Menthol and tobacco-flavored e-cig exposure inhibit fibroblast differentiation markers

We also isolated RNA and protein from HFL-1 after e-cig exposure and measured the expression levels of fibronectin, COL1A1, and α-SMA (Fig. 2). After exposure, the protein abundance of fibronectin was significantly upregulated in the PG/VG group, while significantly decreased in the tobacco flavor group, compared to the air group (Fig. 2A). Significantly decreased protein expression levels of COL1A1 and α-SMA after menthol and tobacco flavored e-cig exposure were observed (Fig. 2A). Similarly, we also noticed a significantly decreased transcript level of *ACTA2* after menthol and tobacco-flavored e-cig exposure (Fig. 2B). The gene expression of COL1A1 was significantly increased after the PG/VG group compared to the air group, while no significant differences were found between menthol vs. air, or tobacco vs. air (Fig. 2B). Non-significant increased trend was noticed in the RNA level of *FNI* in PG/VG group compared to air group, and there is no altered gene expression of *FNI* in the menthol or tobacco exposure group compared to air group (Fig. 2B). Protein abundance and distribution of COL1A1 was also detected by immunofluorescence staining, which showed uniform distribution of COL1A1 in either air group or PG/VG exposed group, while diminished protein expression of COL1A1 was noticed after menthol and tobacco flavored e-cig exposure (Fig. 2C). Full blots are given in Suppl Fig. 1.

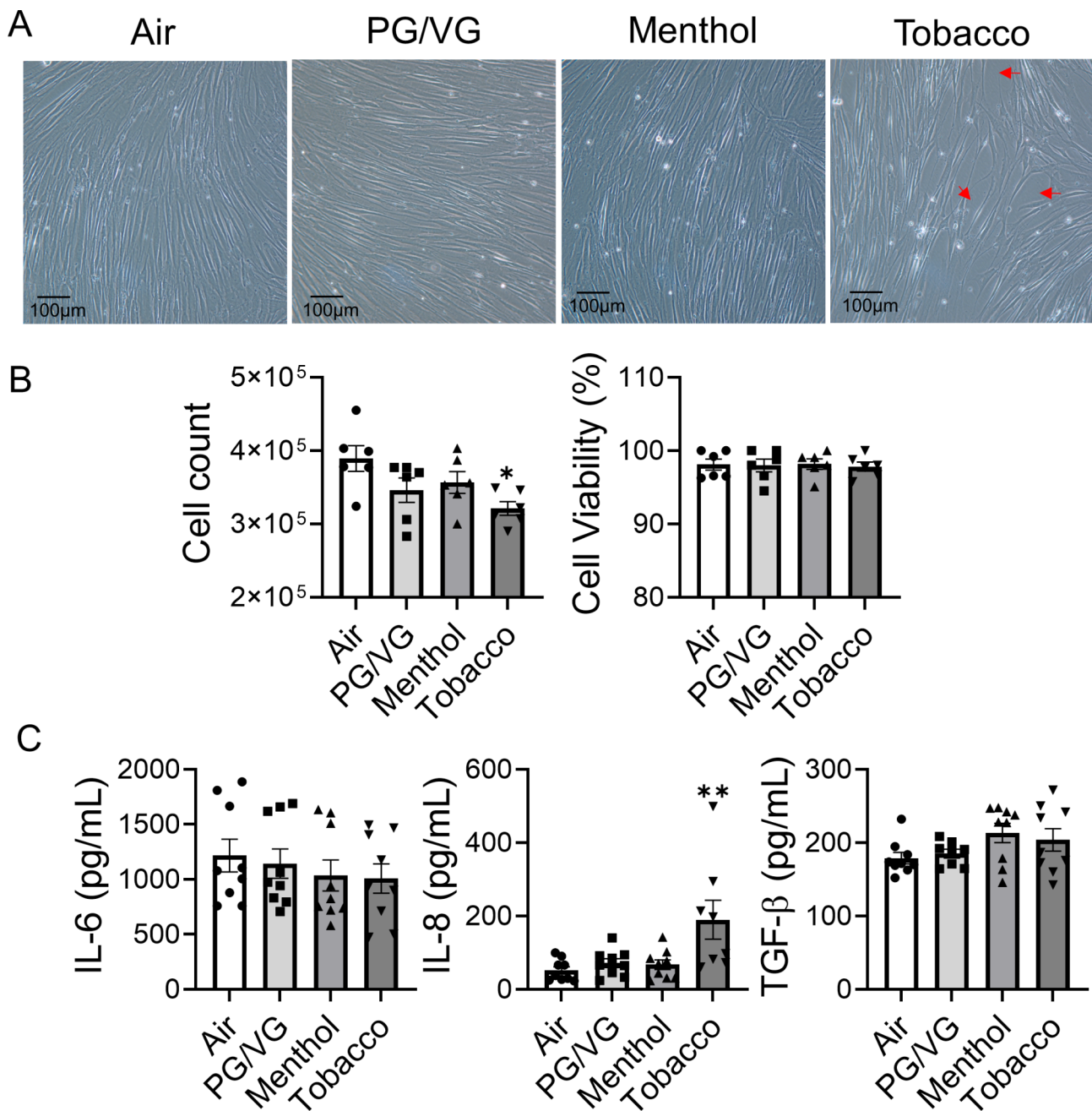


Fig. 1 Tobacco flavored e-cig induced inflammatory responses in lung fibroblast HFL-1 cells exposed to air, PG/VG, or tobacco flavored e-cig for 10 min, and then cultured for 2 days. **(A)**. Representative pictures of HFL-1 cells were taken under 20x microscope. **(B)**. Cell number and viability was measured by AO/PI staining. **(C)** Conditioned medium was collected for IL-6, IL-8 and TGF-β analysis. Data presented as mean ± SEM (n=6–9. * P < 0.05, ** P < 0.01, vs. air)

Tobacco-flavored e-cig exposure inhibit wound healing ability and contractility in HFL-1

Since the fibroblast differentiation markers were inhibited after menthol and tobacco-flavored e-cig exposure, we would like to determine the wound healing ability of HFL-1 after menthol and tobacco-flavored e-cig exposure (Fig. 3). We generated the wound scratch before e-cig exposure, and then exposed the scratched cells to PG/

VG, menthol-flavored e-cig, and tobacco-flavored e-cig. Tobacco-flavored e-cig exposure slowed down the healing rate of the migration of fibroblasts into the wounded area, while no difference after PG/VG and menthol-flavored e-cig exposure was found compared to air group (Fig. 3). We also applied HFL-1 to form a microtissue for measuring the differentiated contractility after exposure to PG/VG, menthol-flavored, and tobacco-flavored e-cigs

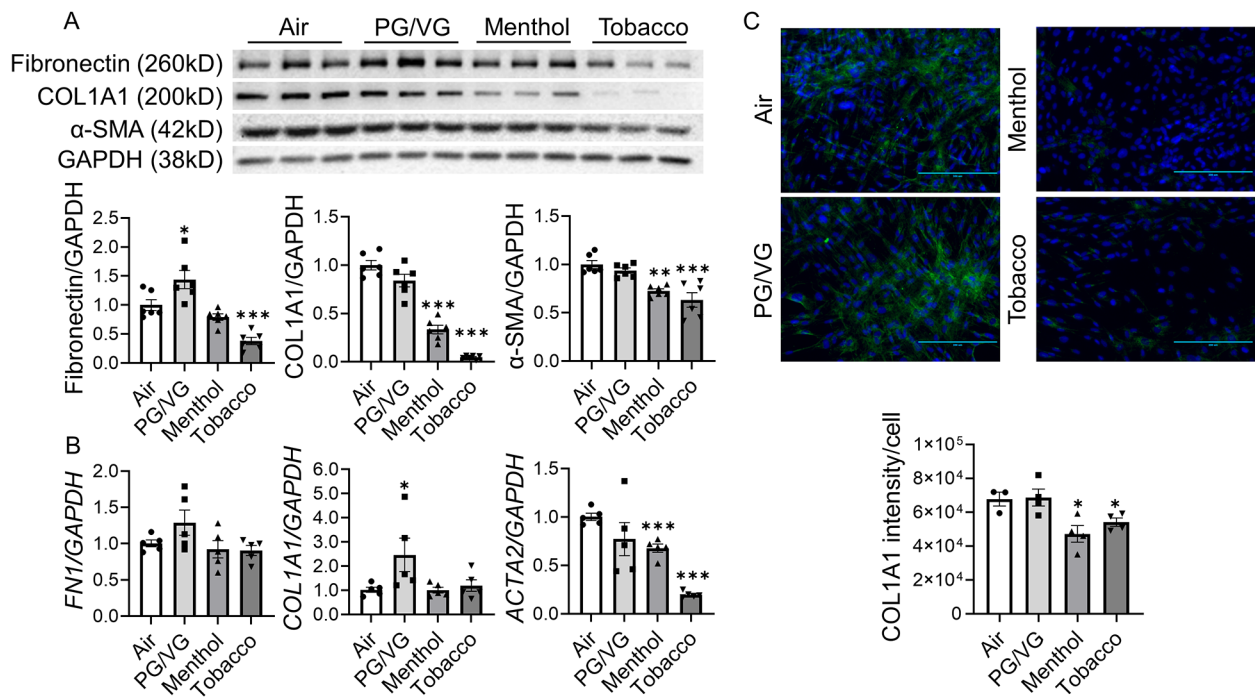


Fig. 2 Tobacco flavored e-cig inhibited fibroblast differentiation markers

HFL-1 cells exposed to air, PG/VG, and tobacco flavored e-cig for 10 min, and then cultured for 2 days. **(A)** cells were lysed and protein was isolated for western blotting, fibronectin, COL1A1, and αSMA were analyzed, GAPDH was used as the endogenous control. **(B)**. RNA was isolated from cells, and *FN1*, *COL1A1*, and *ACTA2* were measured by qRT-PCR, GAPDH was used as the endogenous control. **(C)** Cells were fixed, and stained with COL1A1, the fluorescence intensity was measured by EVOMS, fluorescence intensity /cell was calculated via ImageJ. Data presented as mean ± SEM. (n = 3–6. * P < 0.05, ** P < 0.01, *** P < 0.001 vs. air). Scale bar = 200 μm

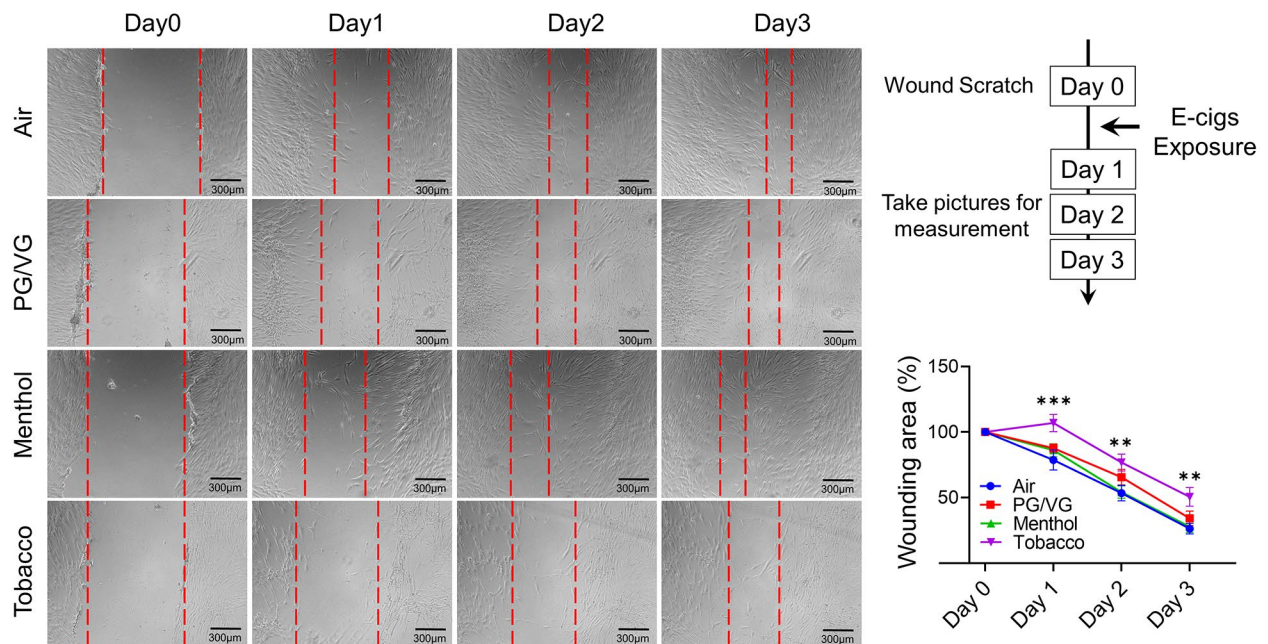


Fig. 3 Tobacco flavored e-cigs inhibited wound healing mediated by lung fibroblast

HFL-1 cells were scratched and then exposed to air, PG/VG, or tobacco flavored e-cig for 10 min, and then cultured for 2 days. The scratched wounds were monitored by taking pictures under the microscope daily. The same position has been selected by recording the coordinates from Cytation 5 imaging system. Data presented as mean ± SEM. (n = 11–12. * P < 0.05, ** P < 0.01, vs. air)

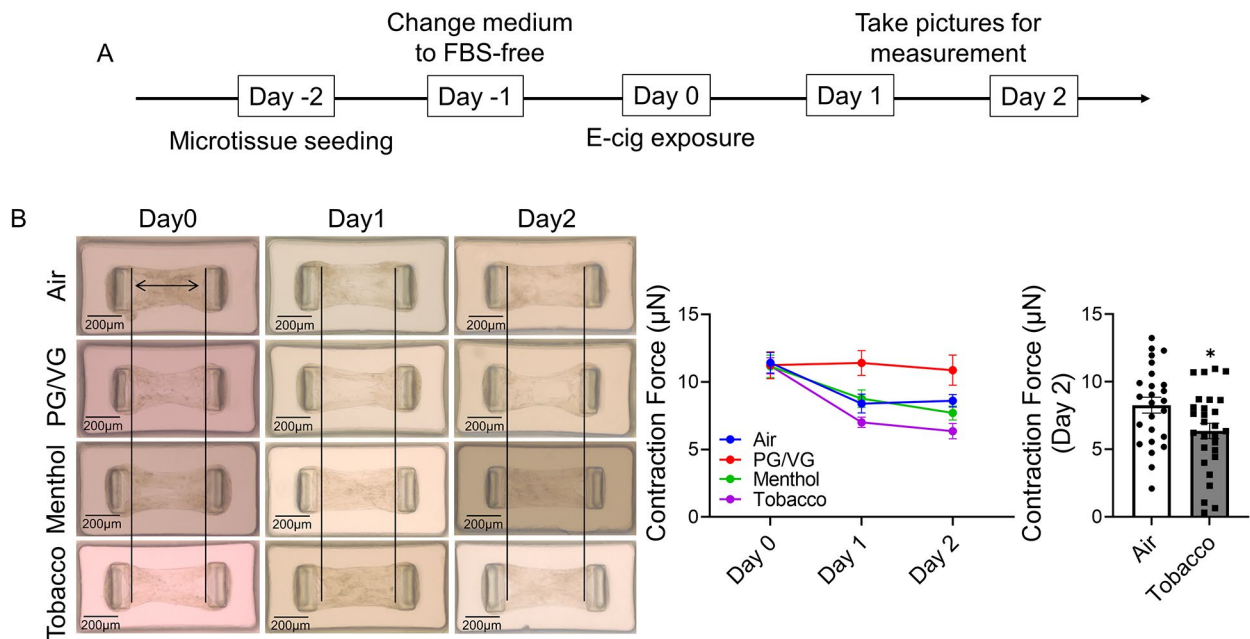


Fig. 4 Tobacco flavored e-cig exposure decreased the contraction force of HFL-1 formed tissue

(A). HFL-1 cells were used to form microtissue first, then exposed to air, PG/VG, and tobacco flavored e-cig for 10 min, and followed with 2 days culture. (B). The individual pictures of microtissue were taken by microscope for measurement of contraction force. Data presented as mean \pm SEM. ($n \geq 10$. * $P < 0.05$ vs. Air)

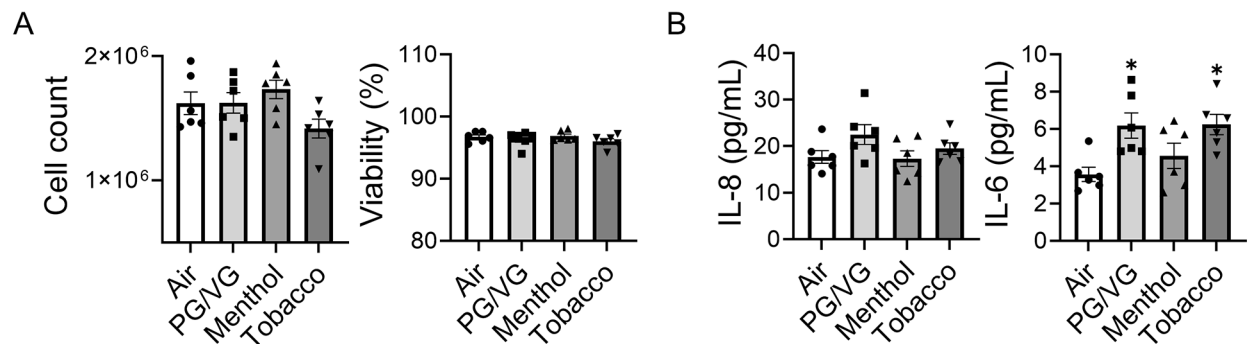


Fig. 5 Unflavored and Tobacco flavored e-cig induced inflammatory responses in lung bronchial epithelium

BEAS-2B cells exposed to air, PG/VG, and tobacco flavored e-cig for 10 min, and then cultured for 2 days. (A). Cell number and viability was measured by AO/PI staining/ (B) Conditioned medium was used for IL-6 and IL-8 analysis. Data presented as mean \pm SEM ($n = 6$. * $P < 0.05$ vs. air)

(Fig. 4A). Decreased contraction force was observed in air, menthol, and tobacco-flavored e-cig exposure groups after exposure, while the PG/VG group showed no altered contraction force during 2 days of culture (Fig. 4B). At day 2 post-exposure, tobacco-flavored e-cig exposure showed a significantly decreased contraction force compared to the air group (Fig. 4B).

Flavored e-cig exposure induced inflammatory responses and epithelial-mesenchymal transition (EMT) in BEAS-2B

We also exposed BEAS-2B to PG/VG, menthol-, and tobacco-flavored e-cigs for 2 days, no significant difference was observed in cell count and viability (Fig. 5A).

Despite no significant difference in IL-8 level among different treatment groups, the released IL-6 level was increased after PG/VG and tobacco-flavored e-cig exposure compared to the air group (Fig. 5B). RNA and protein were also isolated to identify EMT activation after e-cig exposure (Fig. 6). The gene expression of *CDH1*, *OCLN1*, *TJP1* and *CDH2* were decreased after menthol-flavored e-cig exposure compared to the air group, and non-significant increased transcript levels of *VIM* and *SERPINE1* were identified after the menthol group compared to the air group (Fig. 6A). Tobacco-flavored e-cig exposure showed increased gene expression of *CDH2* while no alteration in other gene expressions (Fig. 6A).

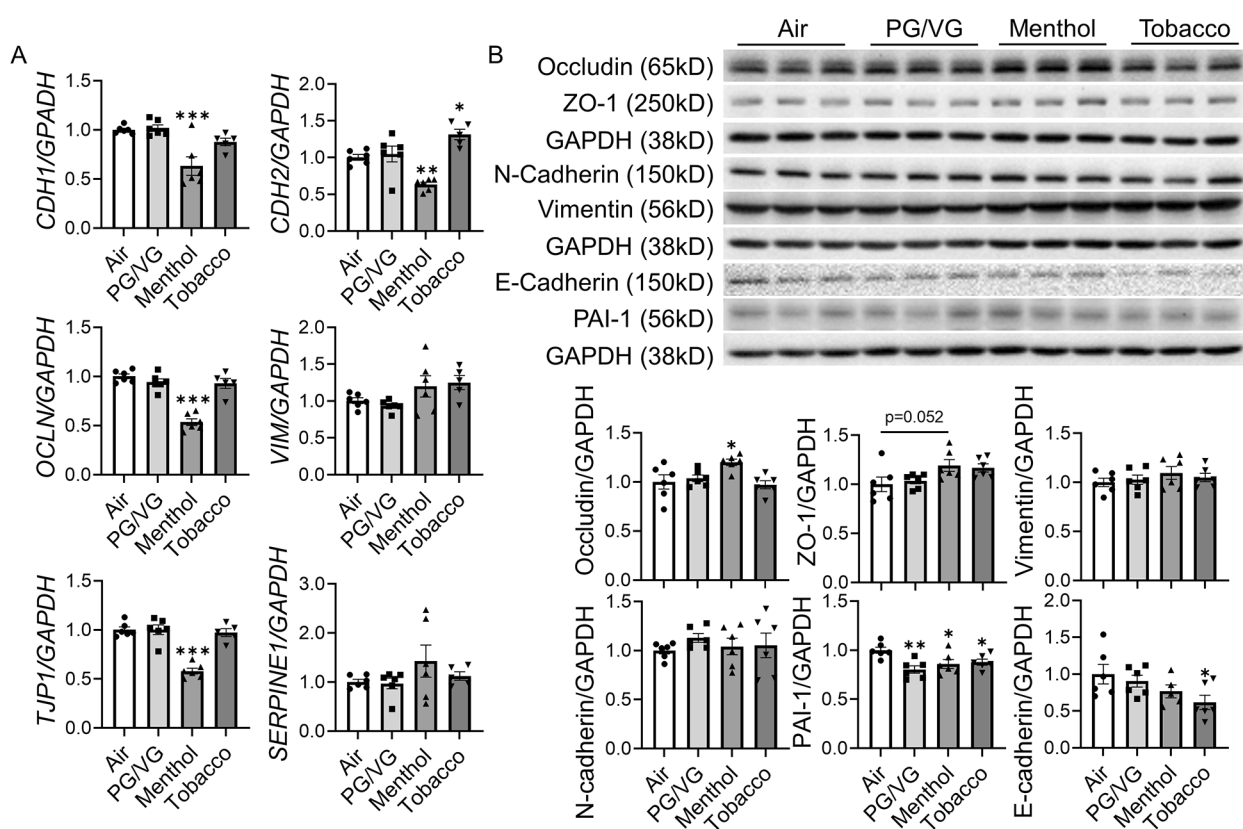


Fig. 6 Flavored e-cig dysregulated EMT in lung bronchial epithelium

BEAS-2B cells exposed to air, PG/VG, and tobacco flavored e-cig for 10 min, and then cultured for 2 days. **(A)** Cells were lysed and RNA was isolated. The gene expression levels of *CDH1*, *CDH2*, *OCLN*, *VIM*, *TJP1*, and *SERPINE1* were measured by qRT-PCR, and *GAPDH* was used as the endogenous control. **(B)** Protein was isolated and expression levels of Occludin, ZO-1, Vimentin, N-cadherin, PAI-1, and E-cadherin were measured by western blot. *GAPDH* was used as the endogenous control for both RNA and protein normalization. Data presented as mean \pm SEM. (n = 5–6. * P < 0.05, ** P < 0.01, *** P < 0.001 vs. air)

There was no difference in protein abundance of vimentin, n-cadherin, and ZO-1 in PG/VG, menthol and tobacco groups compared to air group, while a slightly increased protein level of ZO-1 was identified after menthol-flavored e-cig exposure without significance (Fig. 6B). Increased protein abundance of occludin was found after menthol-flavored exposure, while decreased protein expressions of PAI-1 and E-cadherin were identified after tobacco-flavored e-cig exposure (Fig. 6B). Moreover, decreased protein abundance of PAI-1 was also noticed after PG/VG and menthol-flavored e-cig exposure (Fig. 6B). Full blots are given in Suppl Figs. 2–4.

Discussion

E-cig vaping has been proven to induce lung inflammation and potential tissue remodeling either in acute or chronic exposed mice, and adverse health effects occurred regardless of whether nicotine existed in e-liquid [13, 14]. Various merchandise have been labeled as nicotine-free e-cigs with various flavors to minimize the harmful effects of nicotine vaping, which have been

established by various models [26]. To investigate the health risk of nicotine-free products, we showed that both menthol and tobacco flavored e-cig, either with or without nicotine, presented with suppression on immune and inflammatory responses in mice [27]. Another study showed that nicotine-free e-cig aerosol exposure induced inflammation responses in small airway epithelium [28]. Interestingly, exposure to nicotine-free e-cigs showed different results in vivo and in vitro, indicating that immune responses to e-cig aerosol are cell type-specific. In this study, we identified that lung fibroblast and epithelium exposed to nicotine free tobacco flavored e-cig showed increased inflammatory responses and both tobacco and menthol flavored e-cig exposure interrupted wound healing ability.

Our results showed that tobacco-flavored e-cig exposure decreased cell number and upregulated released IL-8 levels. Inflammatory responses were induced by tobacco-flavored e-cig while PG/VG exposure showed no significant difference compared to the air control. Our results indicate that flavoring chemicals used to prepare

tobacco-flavored e-cigs induce inflammation and cytotoxicity to lung fibroblast, while the humectant does not cause a response. Our recent study showed that one of the tobacco flavoring chemicals, eugenol, showed inflammatory activation on macrophages in a dose-dependent manner [29]. Other tobacco flavoring chemicals, such as coumarin, pentanedione, and maltol, have also been tested and showed significant cytotoxicity and induced oxidative stress in monocytes [10, 12, 30]. Previous studies further corroborate our results showing that tobacco flavoring chemicals used in tobacco-flavored e-cig dominated the inflammatory responses, while the humectant, PG/VG, showed no effect in activating inflammatory progression. However, we also noticed that both PG/VG and tobacco-flavored e-cig exposure showed increased IL-8 levels from lung epithelium. The inflammatory response from lung epithelium was from PG/VG itself, while tobacco flavoring chemicals used in e-liquid did not contribute to inflammation. We believe that the chemicals used to generate tobacco flavor could be diacetyl, acetoin, maltol, or eugenol. Our previous study showed the inflammatory responses from lung epithelium and fibroblast with a dose-dependent response after treatment of diacetyl, acetoin, and maltol [7]. We also showed that eugenol induced inflammation responses in monocytes [10]. We perceive that the chemicals released from tobacco-flavored e-cigs induced cytotoxicity in lung fibroblast, hence inhibiting the wound healing ability. Understanding the toxicology profiles of different flavorants used in e-cig is necessary to regulate tobacco-flavored e-cig products, particularly the presence of any flavoring chemicals used. The different inflammatory responses between lung epithelium and fibroblast confirmed that immune responses induced by e-cig aerosol exposure are cell type-specific. An *in vivo* exposure model with single-cell omics techniques would be helpful to understand the toxicology profile with cell-type specificity.

Besides inflammation, our previous study also showed that flavored e-cig exposure induced dysregulated repair and premature senescence in lung fibroblast [22]. In this study, we tested the wound healing ability of lung fibroblast after being exposed to menthol and tobacco-flavored e-cig. We noticed that the exposure of PG/VG showed increased gene and protein levels of fibronectin and COL1A1, which are the hallmarks of fibroblast differentiation. Our results agreed with a previous study that treatment of PG/VG increased the level of secreted COL1A1, which is even comparable to the TGF- β treatment group [23]. We also showed PG only exposure either acutely or chronically, showed potential dysregulated repair and remodeling in mice lung [13, 14]. Another report described that e-cig users showed logical trend of development of small airway fibrosis [28].

Both human and mouse models have indicated that e-cig exposure could lead to the development of fibrotic diseases while our study pointed that humectants used in e-liquid might be one of the major reasons.

Although the PG/VG exposure showed the activation of fibroblast differentiation which is required during wound healing, menthol, and tobacco-flavored e-cig exposure showed significant inhibition of the protein levels of fibronectin and COL1A1, and both protein and gene abundances of α -SMA. Flavoring chemicals used in both menthol and tobacco-flavored e-liquids inhibit the differentiation markers, indicating inhibited wound healing ability. The scratch assay and microtissue chips in this study further confirmed that tobacco-flavored e-cig inhibited the wound healing ability mediated by lung fibroblast. Other studies also described that e-cig exposure slowed the wound healing process. We have shown that nicotine treatment could inhibit the TGF β -induced fibroblast differentiation and wound recovery [23]. Another report described that mint, menthol, vanilla, and fruit-flavored e-cig inhibited endothelium-mediated wound healing [31]. Exposure to e-cig aerosol also slowed the wound healing process on dermal cells, which showed even worse wound recovery than exposure to conventional cigarette smoke [32]. The flavoring chemicals used for tobacco are diacetyl, acetoin, maltol, or eugenol are GRAS defined by FDA, which considered ingested safely [10–12]. We previously showed dose-dependent inflammatory responses after treatment of diacetyl, acetoin, and maltol [33] and the inflammation responses induced by eugenol in monocytes [29]. The chemical released from tobacco flavorants induced cytotoxicity could be one of the factors inhibiting wound healing in fibroblast. Future experiments investigating the inhalation toxicology profiles of individual GRAS flavorant is necessary to provide primary evidence for regulating tobacco-flavored e-cig products.

In this study, the purpose of using the nicotine-free products are: (1) currently, lots of products are available as labeled nicotine-free e-cigs on the market, and advertised as having no addiction risk; (2) Different flavors are added to e-liquid to increase the appeal of e-cig to users, including the youths; (3) FDA regulates both tobacco-derived nicotine and tobacco-free nicotine, however, there is no regulation of nicotine-free e-cigs while lots of products are on the market, and the inhalation toxicity is not known for these products. Hence, the toxicology profiling of nicotine-free products is necessary to provide evidence for making a policy of regulating non-nicotine e-cigs, or the flavors used in nicotine products. Hence, we have focused on nicotine-free e-cig products in this study, tried to assess the toxicology profiles of different types of nicotine-free e-cigs currently available in the market.

There are limited studies demonstrating the impact of e-cig vaping on dysregulated repair and wound healing, especially nicotine free, flavored e-cigs. This study indicated that tobacco flavored nicotine free e-cig exposure inhibits the wound healing process, fibroblast differentiation, and decreases fibroblast contractility. The inhibited wound healing process due to e-cig vaping could exacerbate lung injury that occurs as a second hit.

Previous research has shown that prior e-cig vaping decreased the survival rate of mice after influenza A Virus (IAV) infection with more bodyweight loss compared to air group [18]. It is clear that IAV infection induced inflammation and immune responses were augmented after e-cig exposure [18]. Similar trends were also identified from the human ex vivo model that precision-cut lung slices (PCLS) from healthy donors showed fewer inflammation responses after IAV infection than PCLS from e-cig users [34]. As expected, prior e-cig vaping increased the severity of SARS-CoV-2 infection [35]. It is well known that e-cig exposure results in inflammatory responses, which is one of the reasons for lung injury exacerbation after IAV infection. Our study showed that inhibited wound healing ability after e-cig could delay the injury repairing and serve as one of the factors for causing prolonged lung damage and contribute to the development of chronic lung diseases.

Conclusion

In conclusion, our results showed that tobacco-flavored nicotine-free e-cig exposure induced inflammation and cytotoxicity in lung fibroblast and epithelium and inhibited wound healing ability with decreased fibroblast differentiation markers and contractility. Inhibited wound healing capacity and pro-inflammatory responses induced by flavored e-cig exposure could be a key factor of lung injury exacerbation when challenged by other environmental hazards.

Abbreviations

e-cig	Electronic cigarette
PG	Propylene glycol
VG	Vegetable glycerine
COL1A1	Type 1 collagen
α SMA	α -smooth-muscle actin
ENDS	Electronic nicotine delivery systems
GRAS	Generally recognized as safe
MMPs	Matrix metalloproteinases
ADAMs	A disintegrin and metalloprotease
ECM	Extracellular matrix
HFL-1	Human lung fibroblast
BEAS-2B	Human bronchial epithelial cell
PCLS	Precision-cut lung slices

Supplementary Information

The online version contains supplementary material available at <https://doi.org/10.1186/s12931-023-02537-9>.

Supplementary Material 1: Full western blot images reflecting all blots/bands are given in Suppl Fig.

Authors' contributions

Writing – original draft preparation, QW, JL, CP, RZ, IR; writing – review and editing, QW, IR; preparation of schematics, data generation, and conceptual diagrams, QW, JL, CP; supervision, editing, IR; project administration, IR; funding acquisition and compilation, IR. All authors have read and agreed to the published version of the manuscript.

Funding

WNY Center for Research on Flavored Tobacco Products (CRoFT) # U54CA228110 (I.R.), NHLBI # R01HL163428 (R.Z.) and NHLBI # R33HL154117 (R.Z.).

Data Availability

The data and materials will be available upon request.

Declarations

Ethics approval and consent to participate

Not applicable.

Consent for publication

Not applicable.

Competing interests

The authors declare that they have no known competing financial interests or personal relationships that could have appeared to influence the work reported in this article.

Received: 8 June 2023 / Accepted: 14 September 2023

Published online: 10 January 2024

References

1. Farsalinos KE, Polosa R. Safety evaluation and risk assessment of electronic cigarettes as tobacco cigarette substitutes: a systematic review. *Ther Adv Drug Saf.* 2014;5:67–86.
2. Javed F, Kellesarian SV, Sundar IK, Romanos GE, Rahman I. Recent updates on electronic cigarette aerosol and inhaled nicotine effects on periodontal and pulmonary tissues. *Oral Dis.* 2017;23:1052–7.
3. Grana R, Benowitz N, Glantz SA. E-cigarettes: a scientific review. *Circulation.* 2014;129:1972–86.
4. Cheng T. Chemical evaluation of electronic cigarettes. *Tob Control.* 2014;23(Suppl 2):ii11–17.
5. Kaur G, Muthumalage T, Rahman I. Mechanisms of toxicity and biomarkers of flavoring and flavor enhancing chemicals in emerging tobacco and non-tobacco products. *Toxicol Lett.* 2018;288:143–55.
6. Park-Lee E, Ren C, Cooper M, Cornelius M, Jamal A, Cullen KA. Tobacco Product Use among Middle and High School Students - United States, 2022. *MMWR Morb Mortal Wkly Rep.* 2022;71:1429–35.
7. Diaz MC, Donovan EM, Schillo BA, Vallone D. Menthol e-cigarette sales rise following 2020 FDA guidance. *Tob Control.* 2021;30:700–3.
8. Jensen RP, Luo W, Pankow JF, Strongin RM, Peyton DH. Hidden formaldehyde in e-cigarette aerosols. *N Engl J Med.* 2015;372:392–4.
9. Jensen RP, Strongin RM, Peyton DH. Solvent Chemistry in the electronic cigarette reaction vessel. *Sci Rep.* 2017;7:42549.
10. Allen JG, Flanigan SS, LeBlanc M, Vallarino J, MacNaughton P, Stewart JH, Christiani DC. Flavoring chemicals in E-Cigarettes: Diacetyl, 2,3-Pentanedione, and Acetoin in a sample of 51 products, including Fruit-, Candy-, and Cocktail-Flavored E-Cigarettes. *Environ Health Perspect.* 2016;124:733–9.
11. Lamb T, Muthumalage T, Meehan-Atrash J, Rahman I. Nose-only exposure to Cherry- and Tobacco-Flavored E-Cigarettes Induced Lung inflammation in mice in a sex-dependent manner. *Toxics* 2022, 10.
12. Omaiye EE, Luo W, McWhirter KJ, Pankow JF, Talbot P. Ethyl maltol, vanillin, corylone and other conventional confectionery-related flavour chemicals

- dominate in some e-cigarette liquids labelled 'tobacco' flavoured. *Tob Control*. 2022;31:238–s244.
13. Wang Q, Ahmad Khan N, Muthumalage T, Lawyer GR, McDonough SR, Chuang T-D, Gong M, Sundar IK, Rehan VK, Rahman I. Dysregulated repair and inflammatory responses by e-cigarette-derived inhaled nicotine and humectant propylene glycol in a sex-dependent manner in mouse lung. *FASEB BioAdvances*. 2019;1:609–23.
 14. Wang Q, Sundar IK, Li D, Lucas JH, Muthumalage T, McDonough SR, Rahman I. E-cigarette-induced pulmonary inflammation and dysregulated repair are mediated by nAChR $\alpha 7$ receptor: role of nAChR $\alpha 7$ in SARS-CoV-2 Covid-19 ACE2 receptor regulation. *Respir Res*. 2020;21:154.
 15. Larcombe AN, Janka MA, Mullins BJ, Berry LJ, Bredin A, Franklin PJ. The effects of electronic cigarette aerosol exposure on inflammation and lung function in mice. *Am J Physiol Lung Cell Mol Physiol*. 2017;313:L67–L79.
 16. Lamb T, Muthumalage T, Meehan-Atrash J, Rahman I. Nose-Only Exposure to Cherry- and Tobacco-Flavored E-Cigarettes Induced Lung Inflammation in Mice in a Sex-Dependent Manner. In *Toxics*, vol. 10; 2022.
 17. Ito Y, Correll K, Schiel JA, Finigan JH, Prekeris R, Mason RJ. Lung fibroblasts accelerate wound closure in human alveolar epithelial cells through hepatocyte growth factor/c-Met signaling. *Am J Physiol Lung Cell Mol Physiol*. 2014;307:L94–105.
 18. Sussan TE, Gajghate S, Thimmulappa RK, Ma J, Kim JH, Sudini K, Consolini N, Cormier SA, Lomnicki S, Hasan F, et al. Exposure to electronic cigarettes impairs pulmonary anti-bacterial and anti-viral defenses in a mouse model. *PLoS ONE*. 2015;10:e0116861.
 19. Tan KS, Wang Y. Vaping and respiratory viruses: the end for ENDS? *Am J Respir Cell Mol Biol*. 2021;64:16–8.
 20. Martin EM, Clapp PW, Rebuli ME, Pawlak EA, Glista-Baker E, Benowitz NL, Fry RC, Jaspers I. E-cigarette use results in suppression of immune and inflammatory-response genes in nasal epithelial cells similar to cigarette smoke. *Am J Physiol Lung Cell Mol Physiol*. 2016;311:L135–144.
 21. Darby IA, Hewitson TD. Fibroblast differentiation in wound healing and fibrosis. *Int Rev Cytol*. 2007;257:143–79.
 22. Lucas JH, Muthumalage T, Wang Q, Friedman MR, Friedman AE, Rahman I. E-Liquid containing a mixture of Coconut, Vanilla, and Cookie Flavors causes Cellular Senescence and Dysregulated Repair in pulmonary fibroblasts: implications on premature aging. *Front Physiol* 2020, 11.
 23. Lei W, Lerner C, Sundar IK, Rahman I. Myofibroblast differentiation and its functional properties are inhibited by nicotine and e-cigarette via mitochondrial OXPHOS complex III. *Sci Rep*. 2017;7:43213.
 24. Behar RZ, Hua M, Talbot P. Puffing topography and nicotine intake of electronic cigarette users. *PLoS ONE*. 2015;10:e0117222.
 25. Chen Z, Wang Q, Asmani M, Li Y, Liu C, Li C, Lippmann JM, Wu Y, Zhao R. Lung microtissue array to screen the fibrogenic potential of Carbon Nanotubes. *Sci Rep*. 2016;6:31304.
 26. Park J-A, Crotty Alexander LE, Christiani DC. Vaping and lung inflammation and injury. *Annu Rev Physiol*. 2022;84:611–29.
 27. Muthumalage T, Rahman I. Pulmonary immune response regulation, genotoxicity, and metabolic reprogramming by menthol- and tobacco-flavored e-cigarette exposures in mice. *Toxicol Sci* 2023.
 28. Gellatly S, Pavelka N, Crue T, Schweitzer KS, Day BJ, Min E, Numata M, Voelker DR, Scruggs A, Petrache I, Chu HW. Nicotine-free e-Cigarette vapor exposure stimulates IL6 and mucin production in human primary small Airway Epithelial cells. *J Inflamm Res*. 2020;13:175–85.
 29. Lamb T, Rahman I. Pro-inflammatory effects of aerosols from e-cigarette-derived flavoring chemicals on murine macrophages. *Toxicol Rep*. 2023;10:431–5.
 30. Muthumalage T, Prinz M, Anshar KO, Gerloff J, Sundar IK, Rahman I. Inflammatory and oxidative responses Induced by exposure to commonly used e-Cigarette flavoring chemicals and flavored e-Liquids without Nicotine. *Front Physiol*. 2017;8:1130.
 31. Liu Z, Zhang Y, Youn JY, Zhang Y, Makino A, Yuan JX, Cai H. Flavored and nicotine-containing E-Cigarettes induce impaired angiogenesis and Diabetic Wound Healing via increased endothelial oxidative stress and reduced NO bioavailability. *Antioxid (Basel)* 2022, 11.
 32. Troiano C, Jaleel Z, Spiegel JH. Association of electronic cigarette vaping and cigarette smoking with decreased Random Flap viability in rats. *JAMA Facial Plast Surg*. 2019;21:5–10.
 33. Gerloff J, Sundar IK, Freter R, Sekera ER, Friedman AE, Robinson R, Pagano T, Rahman I. Inflammatory response and barrier dysfunction by different e-Cigarette Flavoring Chemicals identified by Gas Chromatography-Mass Spectrometry in e-Liquids and e-Vapors on Human Lung epithelial cells and fibroblasts. *Appl in Vitro Toxicol*. 2017;3:28–40.
 34. Agraval H, Crue T, Schaunaman N, Numata M, Day BJ, Chu HW. Electronic cigarette exposure increases the severity of Influenza A Virus infection via TRAIL dysregulation in Human Precision-Cut lung slices. *Int J Mol Sci* 2023, 24.
 35. Schweitzer K, Cornell C, Egersdorf N, Bosco-Lauth A, Majka S, Groshong S, Chu H, Bridges J, Bowen R, Downey G. Impact of Influenza Virus and E-cigarette Vaping Pre-Exposures on Outcomes of SARS-CoV-2 infection in Hamster. B62 E-CIGARETTES AND VAPING: ANIMAL AND CELL CULTURE MODELS. *American Thoracic Society*; 2022: A5660–0.

Publisher's Note

Springer Nature remains neutral with regard to jurisdictional claims in published maps and institutional affiliations.